



Measurement of the
 $e^+e^- \rightarrow \Lambda\bar{\Lambda}$ cross section from threshold to 3.00
GeV using events with
initial-state radiation

--Phys. Rev. D 107, 072005 (2023)

By Wang Yijing



- **Introduction**
- **Event Selection**
- **Background Analysis**
- **Systematic Uncertainty**
- **Result**



For a spin= $\frac{1}{2}$ baryon (B), the cross section in the Born approximation of one-photon-exchange process $e^+e^- \rightarrow B\bar{B}$ is parametrized in terms of electric and magnetic form factors G_E and G_M by

$$\sigma^B(s) = \frac{4\pi\alpha^2 C\beta}{3s} \left[|G_M(s)|^2 + \frac{2m_B^2 c^2}{s} |G_E(s)|^2 \right]$$

Where α is the fine-structure constant, C is the Coulomb correction factor, $\beta = \sqrt{1 - 4m_B^2/s}$, m_B is the mass of the baryon. From this equation, we can get that in the neutral baryon-pair case, the cross section should be zero.

However, there have been many experimental studies on the neutral baryon-pair production cross sections in the past decades. They found there is a step in the production cross section near the threshold.

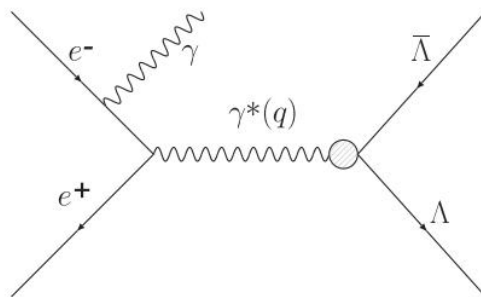
A way has been used to measure the cross section which gets the result by measuring the radiative return channel $e^+e^- \rightarrow \Lambda\bar{\Lambda}\gamma$, where γ is a hard photon from the initial-state radiation (ISR) process.

The differential Born cross section of the two process can be related by the following function:

$$\frac{d\sigma_{e^+e^- \rightarrow \gamma\Lambda\bar{\Lambda}}(q^2)}{dq^2} = \frac{1}{s} W(s, x) \sigma_{\Lambda\bar{\Lambda}}(q^2)$$

Here, $x=1-\frac{q^2}{s}$, $W(s, x)$ is a very complex function, which describes the probability for the emission of an ISR photon.

In this analysis, we present the measurement of the $e^+e^- \rightarrow \Lambda\bar{\Lambda}$ cross section from the production threshold up to $3.00\text{GeV}/c^2$ using the ISR process.





The complete process we study is $e^+e^- \rightarrow \gamma\Lambda\bar{\Lambda} \rightarrow \gamma(p\pi^-(\bar{p}\pi^+))$, where γ is the ISR photon. We categorize the reconstruction of signal candidates into two modes:

Mode1: Fully reconstructed events.

Mode2: A partial reconstruction method with a missing pion .

Charged Tracks:

1. The charged tracks detected in (MDC) are required to be within $|\cos \theta| < 0.93$, where θ is the polar angle with respect to the z axis.
2. $d_z < 30$ cm and $d_t < 10$ cm , where d is the distance of closest approach of each charged track to the interaction point
3. For each signal candidate, at least three charged tracks are required.

PID:

The combined information of dE/dx and TOF is used to calculate particle identification (PID) probabilities .

Second Vertex Fit

The candidate is reconstructed by fitting the $(p\pi^-)(\bar{p}\pi^+)$ tracks to a common decay vertex.

The reconstructed mass of the $\Lambda(\bar{\Lambda})$ satisfy $|M_{\Lambda(\bar{\Lambda})} - m_{\Lambda(\bar{\Lambda})}| < 6.46 \text{ MeV}/c^2$

Selection By EMC Shower

1. The shower time is within 700 ns of the event's start time t .
2. A photon candidate is selected if its deposited energy is greater than 0.4 GeV.
3. For each candidate signal event, at least one photon is required which is considered as the ISR photon.

Kinematic Fit

1. Mode I : a four-constraint (4C) kinematic fit requiring energy momentum conservation under the hypothesis of a $\gamma\Lambda\Lambda^-$ final state is applied to the signal candidates. Also we require $\chi^2_{4C} \leq \chi^2_{4C\gamma\gamma}$.

2. Mode II: besides the fit 4c, a fit 1c is applied. The $\gamma\bar{p}(\gamma p)$ combination with the minimum χ^2_{1C} is selected. We require $\chi^2_{4C} \leq 50$, ($\chi^2_{1C} \leq 5$).

3. $M_{\text{miss}\pi}$: $0.012 \leq M^2_{\pi} \leq 0.025 \text{ GeV}^2/c^4$ is applied.



Events of $e^+e^- \rightarrow \pi_0\Lambda\bar{\Lambda}$

: A data-driven method is used to estimate their contribution. The sideband regions are chosen in the distribution of the invariant mass of $\gamma\gamma$ ($M_{\gamma\gamma}$). The number of events of this sample is calculated by $N_{\text{data}\pi_0} = N_{\text{SigReg}\pi_0} - N_{\text{Side}\pi_0}/2$.

Next, the contribution from the remaining background ($N_{\text{bkg}\pi_0}$) in the signal candidates is determined by

$$N_{\pi^0}^{\text{bkg}} = N_{\pi^0}^{\text{data}} \times \frac{N_{\text{ISR}}^{\text{MC}}}{N_{\pi^0}^{\text{MC}}}$$

Events of $e^+e^- \rightarrow \gamma(\Lambda\bar{\Sigma}_0 + \text{c.c.})$

We use a MC sample.

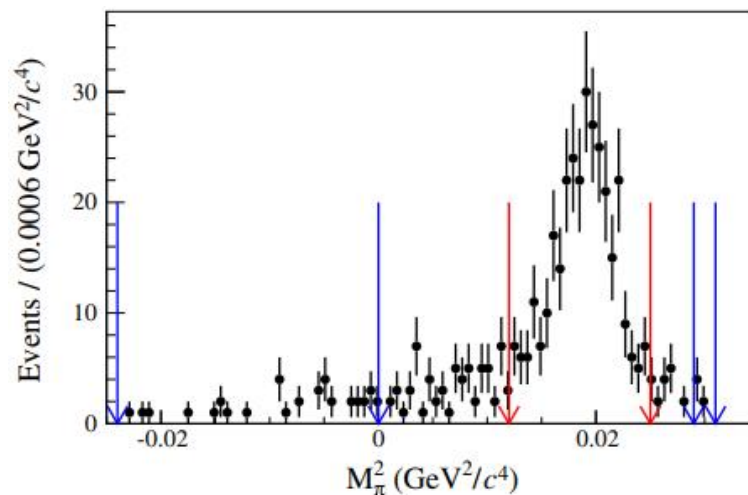
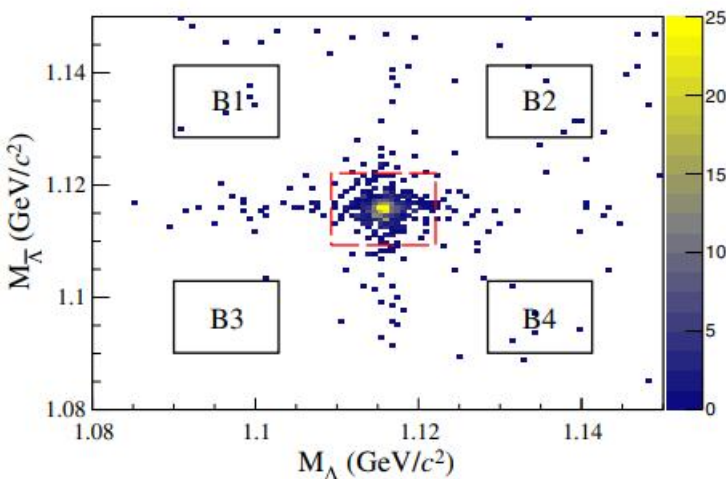
A scaling factor is obtained by $f = N_{\text{exp}}/N_{\text{gen}}$, the number of background events are estimated by

$$N_{\Lambda\Sigma}^{\text{bkg}} = f \times N_{\Lambda\Sigma}^{\text{MC}}$$

Non- $\Lambda(\bar{\Lambda})$ background.

Mode I :two-dimensional (2D) sideband regions of M_Λ versus $M_{\bar{\Lambda}}$ are adopted

Mode II :one dimensional (1D) sideband regions in the distribution of M_π^2 are used.



The numbers of events from sideband regions of data ($N_{\text{data non-}\Lambda(\bar{\Lambda})}$) are calculated by

$$N_{\text{non-}\Lambda\bar{\Lambda}}^{\text{data}} = \frac{1}{4} \times N_{2\text{D}} + \frac{1}{2} \times N_{1\text{D}}$$

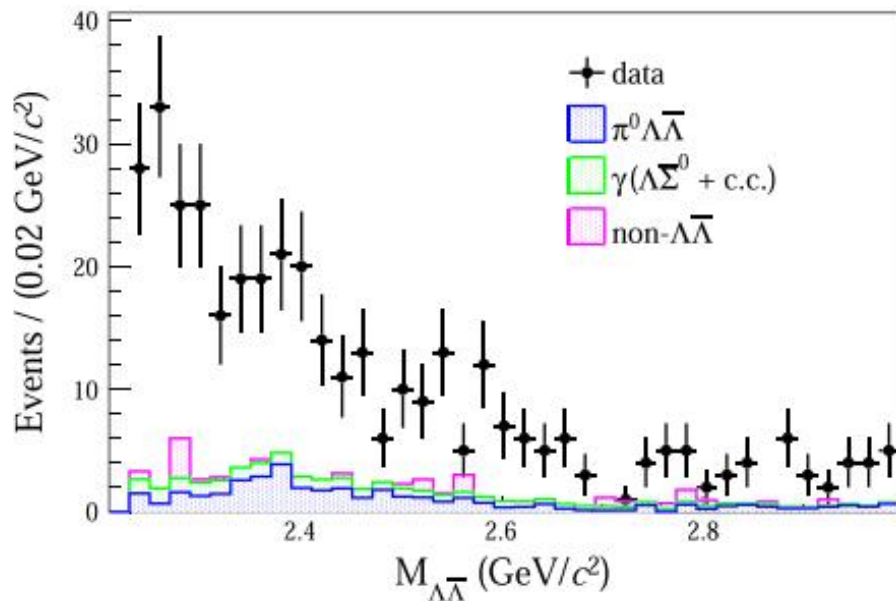
The same sideband regions are used for the other two MC samples .And the number of non- $\Lambda(\bar{\Lambda})$ background events is estimated by

$$N_{\text{non-}\Lambda\bar{\Lambda}}^{\text{bkg}} = N_{\text{non-}\Lambda\bar{\Lambda}}^{\text{data}} - N_{\text{non-}\Lambda\bar{\Lambda}}^{\text{MC}}$$

Background Analysis



Here are the final results :



$M_{\Lambda\bar{\Lambda}}$ (GeV/ c^2)	N_{obs}	$N_{\pi^0}^{\text{bkg}}$	$N_{\Lambda\Sigma}^{\text{bkg}}$	$N_{\text{non-}\Lambda\bar{\Lambda}}^{\text{bkg}}$
2.231–2.250	28.0 ± 5.3	1.9 ± 1.2	1.28 ± 0.05	0.63 ± 0.70
2.25–2.27	32.0 ± 5.7	$0.7^{+0.6}_{-0.5}$	1.35 ± 0.05	$-0.41^{+1.61}_{-0.02}$
2.27–2.29	25.0 ± 5.0	1.4 ± 0.6	1.36 ± 0.05	2.67 ± 1.22
2.29–2.31	24.0 ± 4.9	1.3 ± 0.6	1.37 ± 0.05	0.69 ± 0.71
2.31–2.34	28.0 ± 5.3	2.4 ± 0.7	2.00 ± 0.07	$0.08^{+1.24}_{-0.50}$
2.34–2.37	27.0 ± 5.2	4.2 ± 0.9	1.83 ± 0.05	$0.11^{+1.24}_{-0.50}$
2.37–2.40	34.0 ± 5.8	5.2 ± 0.9	1.54 ± 0.05	$-0.32^{+1.61}_{-0.02}$
2.40–2.44	28.0 ± 5.3	3.5 ± 0.8	1.74 ± 0.05	$0.10^{+1.24}_{-0.50}$
2.44–2.48	23.0 ± 4.8	3.3 ± 0.7	1.53 ± 0.05	$-0.32^{+1.61}_{-0.02}$
2.48–2.52	16.0 ± 4.0	3.3 ± 0.7	1.28 ± 0.05	$1.22^{+1.43}_{-0.87}$
2.52–2.56	19.0 ± 4.4	1.7 ± 0.5	1.01 ± 0.05	1.51 ± 0.90
2.56–2.60	18.0 ± 4.2	1.4 ± 0.5	0.87 ± 0.05	$-0.21^{+1.61}_{-0.02}$
2.60–2.70	24.0 ± 4.9	1.4 ± 0.5	1.74 ± 0.05	$-0.39^{+1.61}_{-0.02}$
2.70–2.80	15.0 ± 3.9	1.5 ± 0.5	1.12 ± 0.04	3.00 ± 1.25
2.80–2.90	15.0 ± 3.9	2.3 ± 0.6	0.73 ± 0.03	$0.07^{+1.17}_{-0.25}$
2.90–3.00	18.0 ± 4.2	2.6 ± 0.7	0.49 ± 0.03	$0.36^{+1.24}_{-0.50}$

The uncertainties are statistical.

The combined results of different reconstructed methods and different datasets are summarized in the following two tables:

Source	Uncertainty
Luminosity	1.1
Λ reconstruction	2.1
$\bar{\Lambda}$ reconstruction	2.8
$\mathcal{B}(\Lambda \rightarrow p\pi)$	1.6
$p(\bar{p})$ tracking and PID	0.7
M_π^2 window	0.6
ISR photon detection	1.0
Kinematic fit	1.7
Neglected background	1.5
Total	4.7

The correlated systematic uncertainties (in %) on the cross section measurement.

$M_{\Lambda\bar{\Lambda}}$ (GeV/ c^2)	$\pi^0\Lambda\bar{\Lambda}$	$\gamma\Lambda\Sigma^0$	non- $\Lambda\bar{\Lambda}$	Ang	MC	Total
2.231–2.250	0.3	0.6	0.4	2.7	1.6	3.2
2.25–2.27	0.1	0.9	1.4	0.6	1.4	2.2
2.27–2.29	0.7	1.8	0.5	2.3	4.1	5.1
2.29–2.31	0.9	1.9	0.4	2.2	0.7	3.1
2.31–2.34	1.3	3.6	0.5	2.7	1.5	4.9
2.34–2.37	0.8	3.0	0.4	1.6	0.9	3.6
2.37–2.40	1.0	2.0	3.3	0.3	0.9	4.1
2.40–2.44	0.6	3.0	0.4	0.8	0.8	3.2
2.44–2.48	0.5	2.4	0.5	1.7	2.2	3.6
2.48–2.52	1.6	5.2	5.2	2.2	2.2	8.2
2.52–2.56	1.0	5.4	0.9	1.7	3.3	6.7
2.56–2.60	0.5	2.9	0.4	0.8	1.8	3.6
2.60–2.70	0.9	3.2	0.9	2.5	1.4	4.4
2.70–2.80	7.1	9.3	24.8	2.1	1.9	27.5
2.80–2.90	1.7	2.3	2.3	2.1	1.5	4.4
2.90–3.00	1.2	1.5	0.3	1.9	5.4	6.0

The systematic uncertainties of different channels.



The integrated luminosity: 0.5% at $\sqrt{S}=3.773$ GeV and 1.0% at other c.m. energies.
The effective luminosity of the ISR process based on $W(s,x)$: 0.5% uncertainty.

Reconstruction of Λ and $\bar{\Lambda}$ (studied by a control sample of $J/\psi \rightarrow pK^- \bar{\Lambda} + c.c$) :
2.8% and 3.8% at $\sqrt{S}=3.773$ GeV ; 2.6% and 3.4% at other energy points
ISR photon detection: 1%

$p(\bar{p})$ tracking and PID : 1.0% for each .

$M^2_{\pi^-}$ ($M^2_{\pi^+}$) window (studied by the control sample of $J/\psi \rightarrow pK^- \bar{\Lambda} + c.c$)
: 1.4% (0.8%) at $\sqrt{S}=3.773$ GeV and 1.5% (0.9%) at other energy points.

The branching fraction of $\Lambda(\bar{\Lambda}) \rightarrow p\pi^- (\bar{p}\pi^+)$: 1.6%.

Kinematic fit :

0.6% (0.6%), 2.6% (2.4%), and 3.3% (3.3%) (all reconstruction, missing π^- , and missing π^+).
Here, the former is for 3.773 GeV, the latter is for other points.



$e^+e^- \rightarrow \pi_0 \Lambda \bar{\Lambda}$ and $e^+e^- \rightarrow \gamma(\Lambda \bar{\Sigma}_0 + \text{c.c.})$;

The larger one of the values of $|\frac{N_{M\gamma\gamma} - N_{3D}}{N_{\text{sig}}}|$ and $|\frac{N_{M\gamma\gamma} - N_{2D}}{N_{\text{sig}}}|$

Non- $\Lambda \bar{\Lambda}$ background:

Move the sideband regions by $0.002 \text{ GeV}/c^2$ and $0.002 \text{ GeV}^2/c^4$ for the 2D and the 1D sidebands. The relative difference between the old and new results is regarded as the uncertainty.

other background channels:

2.2% at $\sqrt{S} = 3.773 \text{ GeV}$ and 1.1% at other energy points.

In this analysis, 12 datasets are used and 3 reconstruction methods are used. We divide the datasets into two groups, $\sqrt{S} = 3.773 \text{ GeV}$ and the second group includes the other datasets at c.m. energies from 4.128 to 4.258 GeV.

Uncertainties are combined as the average value weighted by detection efficiencies. The weighted average formula is

$$\sigma_{\text{tot}}^2 = \sum_{i=1}^{3(2)} \omega_i^2 \sigma_i^2 + \sum_{i,j=1;i \neq j}^{3(2)} \rho_{ij} \omega_i \omega_j \sigma_i \sigma_j,$$

with

$$\omega_i = \frac{\varepsilon_i}{\sum_{i=1}^3 \varepsilon_i} \left(\omega_i = \frac{\varepsilon_i \mathcal{L}_i}{\sum_{i=1}^2 \varepsilon_i \mathcal{L}_i} \right)$$

The cross section for $e^+e^- \rightarrow \Lambda \bar{\Lambda}$ is calculated from the $M_{\Lambda\bar{\Lambda}}$ spectrum by

$$\sigma_{\Lambda\bar{\Lambda}}(M_{\Lambda\bar{\Lambda}}) = \frac{(dN_{\text{sig}}/dM_{\Lambda\bar{\Lambda}})}{\epsilon \cdot \mathcal{B}^2(\Lambda \rightarrow p\pi) \cdot d\mathcal{L}_{\text{int}}/dM_{\Lambda\bar{\Lambda}}}$$

Here are the final results:

$M_{\Lambda\bar{\Lambda}}$ (GeV/ c^2)	N_{sig}	$\bar{\epsilon}$	\mathcal{L} (pb $^{-1}$)	σ (pb)
2.231–2.250	24.1 ± 5.5	0.061	3.95	$245 \pm 56 \pm 14$
2.25–2.27	$30.3^{+5.7}_{-5.9}$	0.062	4.24	$283^{+53}_{-55} \pm 15$
2.27–2.29	19.5 ± 5.2	0.062	4.32	$179 \pm 48 \pm 13$
2.29–2.31	20.7 ± 5.0	0.061	4.41	$190 \pm 46 \pm 11$
2.31–2.34	$23.5^{+5.4}_{-5.5}$	0.059	6.78	$144^{+32.7}_{-33.5} \pm 9.8$
2.34–2.37	$20.8^{+5.3}_{-5.4}$	0.058	6.99	$126.6^{+32.1}_{-32.9} \pm 7.5$
2.37–2.40	$27.6^{+5.9}_{-6.1}$	0.057	7.20	$165^{+35}_{-37} \pm 11$
2.40–2.44	$22.7^{+5.4}_{-5.5}$	0.057	9.95	$98.1^{+23.2}_{-23.7} \pm 5.6$
2.44–2.48	$18.5^{+4.9}_{-5.1}$	0.058	10.37	$75.2^{+19.7}_{-20.8} \pm 4.5$
2.48–2.52	$10.2^{+4.2}_{-4.3}$	0.059	10.82	$38.9^{+15.9}_{-16.5} \pm 3.7$
2.52–2.56	14.7 ± 4.5	0.061	11.30	$52.4 \pm 16.0 \pm 4.3$
2.56–2.60	$15.9^{+4.3}_{-4.6}$	0.063	11.80	$52.1^{+14.0}_{-14.9} \pm 3.1$
2.60–2.70	$21.2^{+4.9}_{-5.2}$	0.066	31.96	$24.6^{+5.7}_{-6.0} \pm 1.6$
2.70–2.80	9.4 ± 4.1	0.070	35.96	$9.1 \pm 4.0 \pm 2.6$
2.80–2.90	$11.9^{+3.9}_{-4.1}$	0.072	40.76	$9.9^{+3.3}_{-3.4} \pm 0.7$
2.90–3.00	$14.5^{+4.3}_{-4.5}$	0.073	46.59	$10.5^{+3.1}_{-3.2} \pm 0.8$

The first uncertainty is statistical and the second is systematic.

We can see that In the first M interval ranging from the threshold up to 2.25 GeV/c² the cross section is determined to be $245 \pm 56 \pm 13$ pb, it is a nonzero value with a statistical significance of 4.3σ . The results are consistent with previous measurements at BABAR and BESIII. We indeed see a step existing near threshold.

